Robust H_∞ Glucose Control in Diabetes Using a Physiological Model

Robert S. Parker and Francis J. Doyle III
Dept. of Chemical Engineering, University of Delaware, Newark, DE 19716

Jennifer H. Ward and Nicholas A. Peppas
Biomaterials and Drug Delivery Laboratories, School of Chemical Engineering, Purdue University,
West Lafayette, IN 47907

A robust H_∞ controller was developed to deliver insulin via a mechanical pump in Type I diabetic patients. A fundamental nonlinear diabetic patient model was linearized and then reduced to a third-order linear form for controller synthesis. Uncertainty in the nonlinear model was characterized by up to $\pm 40\%$ variation in eight physiological parameters. A sensitivity analysis identified the three-parameter set having the most significant effect on glucose and insulin dynamics over the frequency range of interest $\omega = [0.002, 0.2]$ (rad/min). This uncertainty was represented in the frequency domain and incorporated in the controller design. Controller performance was assessed in terms of its ability to track a normoglycemic set point (81.1 mg/dL) in response to a 50 g meal disturbance. In the nominal continuous-time case, the controller maintained glucose concentrations within ± 3.3 mg/dL of set point. A controller tuned to accommodate uncertainty yielded a maximum deviation of 17.6 mg/dL for the worst-case parameter variation.

Introduction

Diabetes mellitus is an incurable disease affecting millions of people worldwide. Type I, or insulin-dependent diabetes mellitus (IDDM), is characterized by insufficient secretion of insulin from the pancreas, resulting in plasma glucose concentrations elevated beyond the normoglycemic range (70–100 mg/dL) (Ashcroft and Ashcroft, 1992). This article examines insulin infusion by mechanical pump as an alternative method to injection therapy. A mechanical device would contain three primary components: a variable rate pump mechanism, which is already on the market in a number of forms (Cohen, 1993; Minimed Corporation, 1999); an *in vivo* glucose sensor, which is an active area of research in the diabetes literature (Preidel et al., 1991; Meyerhoff et al., 1992; Nishida et al., 1995); and a control algorithm, which calculates the necessary insulin delivery rate based on the glucose sensor measurement. This article focuses on the last component.

Early modeling studies of the diabetic condition (Bolie, 1961; Ackerman et al., 1965) established a precedent for

mathematical analysis of insulin-glucose interactions. Later studies utilized more complicated nonlinear models, such as Bergman's "Minimal Model" (Bergman et al., 1981), and incorporated physiological system knowledge in the model structure (Cobelli and Mari, 1983; Sorensen, 1985). From these models, various control algorithms have been developed which typically involved either an implicit or explicit system model and the optimal solution of a quadratic cost functional (Sorensen, 1985; Ollerton, 1989; Fisher, 1991; Parker et al., 1999a). In the synthesis of these controllers, however, the inherent uncertainty in the model has not been explicitly addressed. This could lead to significant performance degradation should the model parameters not represent the actual patient glucose and insulin dynamics.

Significant inter- and intrapatient variability has been documented in the literature (Bremer and Gough, 1999; Puckett and Lightfoot, 1995; Simon et al., 1987; Steil et al., 1994). To obviate the need for complete retuning of the controller for each patient, the control algorithm utilized in an insulin delivery device must be able to compensate for the uncertainty which exists between the internal model and the actual pa-

tient. This clearly motivates the synthesis of a robust control algorithm, and the current work focuses on the H_∞ framework. Previous work on H_∞ controller design for insulin delivery has been performed by Kienitz and Yoneyama (1993). Their work concentrated on controller synthesis from an empirical low-order linear model of the diabetic patient. The current study develops continuous-time H_∞ controllers utilizing the Jacobian linearization of a nonlinear physiologically derived model of the diabetic patient. The motivation for using a detailed nonlinear patient model is the ability to focus the uncertainty characterization on particular tissues or effects which are most responsible for the insulin or glucose variability. The resulting controller is shown to exhibit robust performance to variability in glucose and insulin dynamics.

Patient and Uncertainty Modeling

Nominal model construction

A nonlinear pharmacokinetic/pharmacodynamic compartmental model of the diabetic patient has been constructed previously (Guyton et al., 1978; Sorensen, 1985; Parker, 1999), and is detailed in the Appendix. A meal disturbance model (Lehmann and Deutsch, 1992) was included in the model description. The specific operating conditions for the diabetic patient model used in testing the robust controller algorithms are described in Parker et al. (1999). The diabetic patient model had two inputs and one measured output. Insulin delivery rate, represented as a deviation from its 22.3 mU/min nominal delivery rate, was the manipulated variable (represented as $\bar{u}$). The meal disturbance had a nominal value of 0 mg/min (absorption into the bloodstream), and its signal was referred to as $\bar{m}_d$. Blood glucose concentration, the measured variable, was denoted by $\bar{y}$, and represented the deviation in blood glucose from a nominal value of 81.1 mg/dL. To facilitate controller design, the model inputs and output were scaled such that adequate performance was defined as all signals remaining less than one in magnitude

$$m_d = \frac{1}{360}\bar{m}_d, \quad u = \frac{1}{33.125}\bar{u}, \quad y = \frac{1}{20}\bar{y}$$

Here, the disturbance scaling was determined by its maximum value, and the output scaling by the maximum allowable deviation in glucose concentration. Note that the 20 mg/dL output variation was less than the true constraint (21.1 mg/dL), but this conservatism was warranted given the potential level of uncertainty between either linear model (full-order or reduced) and the nonlinear representation. The scaling for the manipulated input u was based on its expected range.

Linear H_∞ controller synthesis requires a linear system model. The Jacobian linearization of the diabetic patient model was 19th order, which is still burdensome for controller synthesis, as the controller order scales directly with that of the process model. Model reduction was used to generate a low-order process model for use in controller synthesis. From the Jacobian linearization of the nonlinear diabetic patient model, balanced truncation (the *balmr* function in MATLAB, 2000, The MathWorks, Inc.) was used to reduce the model order (Glover, 1984; Moore, 1981). Here, the error introduced by truncating an n-state model, $G(j\omega)$, to a k-
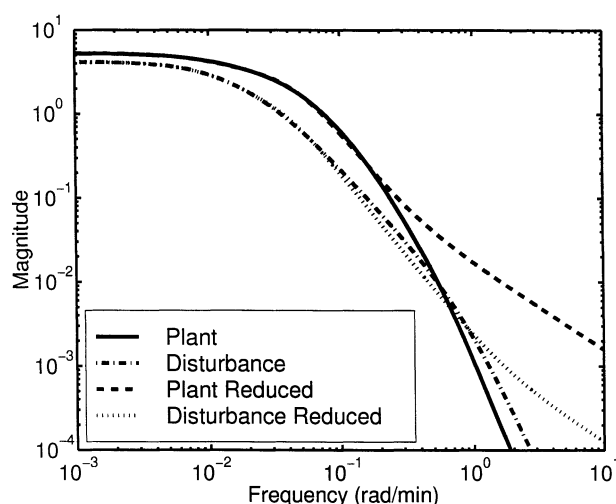

Figure 1. Effect of model reduction on process behavior as a function of frequency.

Full-order (19 state) linear model (patient, solid; disturbance, dash-dot) and reduced-order (3 state) linear model (patient, dashed; disturbance, dotted).

state representation, $G_r(j\omega)$, is given by (Chiang and Safonov, 1992)

$$\| G(j\omega) - G_r(j\omega) \|_\infty = 2 \sum_{i=k+1}^{n} \sigma_i^H \tag{1}$$

where σ_i^H represent the Hankel singular values of the original (full-order) system. In the balanced realization, the relative contribution of a particular state to the process input-output behavior corresponded to the magnitude of its singular value. By truncating the $n-k$ smallest singular values, only those states with comparatively small contribution to the input-output behavior are eliminated. The linear reduced model was given in state-space form as follows

$$\dot{x}_{\text{red}} = A_r x_{\text{red}} + B_r u + B_m m_d \tag{2}$$

$$y = C_r x_{\text{red}} \tag{3}$$

Utilizing linear superposition, the plant could be split further into a pair of single-input single-output (SISO) models: a process model (G), incorporating the manipulated variable (u, insulin) effects, and a disturbance model (G_m), representing the effects of the meal disturbance (m_d). Shown in Figure 1 are the frequency responses of the full-order and reduced SISO models. Performance in the bandwidth region, defined as the portion of the frequency spectrum in which control is effective, was of primary importance. The fastest disturbances affected the patient system with a time constant of approximately 5 min, and the low-frequency behavior was important for steady-state tracking. Hence, the frequency range [0.002, 0.2] was of interest. System behavior in this region was accurately captured by the reduced-order models, as demonstrated in Figure 1. The process model began to exhibit behavioral changes near frequencies of 0.2 rad/min, while the disturbance model showed significant differences in dynamics

at frequencies greater than 1 rad/min. As measurement noise was the only expected process perturbation at high frequency ($>$ 1 rad/min), the 19th-order linear model could be reduced to third order without significantly altering the dynamic behavior in the bandwidth region. This 3-state model was treated as the "nominal" patient, on which controller designs were based.

Uncertainty characterization

Uncertainty due to differences between an actual patient and the diabetic patient model could be related to variations in model parameters. A parametric sensitivity analysis was performed on the full nonlinear model to determine the terms most responsible for changes in blood glucose and insulin dynamics. The glucose and insulin dynamics were found to be most sensitive to variations in the metabolic parameters (Parker et al., 1998). In the patient model, glucose metabolism is mathematically described by threshold functions with the following structure

$$\Gamma_e = E_\Gamma \{ A_\Gamma - B_\Gamma \tanh [C_\Gamma (x_i + D_\Gamma)] \} \qquad (4)$$

Here the subscript i is the state vector element involved in the metabolic effect and the e subscript denotes specific effects within the model, such as the effect of glucose on hepatic glucose production (EGHGP), the effect of glucose on hepatic glucose uptake (EGHGU), or the effect of insulin on peripheral glucose uptake (EIPGU). Inter- or intrapatient uncertainty could be classified physiologically as either a receptor (D_Γ parameter) or post-receptor (E_Γ parameter) defect, and this was modeled mathematically by adjusting the inflection point of the hyperbolic tangent function or the maximum value of Γ_e, respectively. Differences in insulin clearance (metabolism) between patients also existed, and could be modeled as deviations in the fraction of clearance from a given compartment, such as the fraction of hepatic insulin clearance (FHIC) or the fraction of peripheral insulin clearance (FPIC). This uncertainty formulation implied a structured effect of variability on the model, such that the tissues most important to parametric uncertainty were the liver (five parameters) and the peripheral (muscle/fat) tissues (three parameters).

In the absence of physical data from which to identify ranges for parametric variations, it was assumed that $\pm 40\%$ parametric variability in each parameter represented a broad range of potential patients. The exception was FHIC, which was limited to $\pm 20\%$ to guarantee non-negative glucose concentrations. Unfortunately, this level of parametric uncertainty led to greater than 100% model uncertainty at steady-state, such that no linear integrating control algorithm could regulate the process (Morari, 1983). As a subset of the eight parameter problem, the uncertainty was restricted to the three most highly sensitive parameters. Potential correlations between parameters were important, so a systematic method for quantifying model sensitivity to parameter changes was necessary. In this case, sets of three parameters from the possible eight were selected, yielding

$$\binom{8}{3} = 56 \text{ combinations.}$$

Each parameter set was varied in five permutations ($+$max, $+1/2$ max, no change, $-1/2$ max, $-$max) about the nominal values for a total 125 possible variations in each three-parameter set (including the nominal case when no parameters were varied). The nonlinear model was linearized around each of these parameter variations (and their induced state variations), due to the operating point dependent behavior of the patient model, and the resulting linear model was used to determine parametric sensitivity. Uncertainty in the frequency domain, manifested through parameter variations in the 19th-order model, was then measured with respect to the reduced (nominal) model of the diabetic patient over the frequency range of interest, $\omega = [0.002, 0.2]$. This was represented as relative uncertainty (U_{rel}), with the following mathematical description

$$U_{\text{rel}}(\omega) = \left| \frac{G_p(\omega) - G(\omega)}{G(\omega)} \right| \qquad (5)$$

The nominal (three-state) model was given by G, while the set of perturbed models (7,000 total, including duplicates) were evaluated individually and given by G_p. The most sensitive parameter set was therefore identified by summing the relative uncertainty in the frequency range of interest for each perturbation, and then summing over the parameter set. The parameter set which displayed the most significant effect on glucose and insulin dynamics was EIPGU(D_Γ) ($\pm 40\%$ from -5.82), EGHGU(D_Γ) ($\pm 40\%$ from -1.48), and FHIC ($\pm 20\%$ from 0.4) (Parker et al., 1999b).

The 125 perturbed models (G_p) from this parameter set were selected to represent the frequency-domain uncertainty expected in the diabetic patient population. The solid line in Figure 2 shows the upper bound of this relative uncertainty as a function of frequency. This bound was created by taking the maximum uncertainty magnitude of the 125 perturbed patient models at each frequency. Comparatively low uncer-
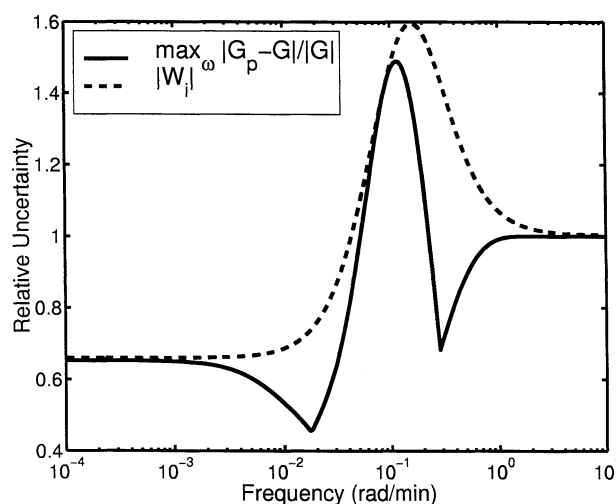
Figure 2. Relative model uncertainty as a function of frequency.

Solid: the upper bound to the 125 perturbed plant (G_p) uncertainties. Dashed: W_i, the multiplicative input uncertainty weight utilized in controller design.

Figure 3. Relative model uncertainty as a function of frequency.

Solid: the upper bound to the 125 perturbed disturbance model (G_m) uncertainties. Dashed: W_{im}, the disturbance multiplicative input uncertainty weight utilized in controller design.

tainty is seen at low frequency increasing beyond the 100% mark near 0.1 rad/min, with an asymptote to 100% uncertainty at high frequency. A similar analysis was performed for the uncertainty in the meal disturbance model (G_m), with results depicted in Figure 3. Here the uncertainty exhibited a local minimum around the bandwidth frequency of 0.2 rad/min, then a relative uncertainty increase with increasing frequency to an asymptote around 10 rad/min.

Continuous-Time H_∞ Controller Synthesis

Theory

The H_∞ control framework is well suited for glucose regulation, due to the ability to tune the controller for robustness to uncertainty while mathematically guaranteeing a certain degree of performance. In this case, it is important for a closed-loop controller to tolerate patient variability and dynamic uncertainty while rapidly rejecting meal disturbances and tracking the constant glucose reference. The controller allowed custom tuning to trade-off these potentially conflicting objectives.

A theoretical derivation of the H_∞ controller synthesis method is beyond the scope of this work. For an overview of state-space H_∞ theory, the reader is referred to (Doyle et al., 1989) and the references therein. The tools used throughout the present controller development are described in (Balas et al., 1995). A block diagram representation of the nominal H_∞ problem is shown in Figure 4, and controllers were synthesized using the methodology in (Skogestad and Postlethwaite, 1996).

A brief overview of H_∞ control and a review of the relevant mathematics is given below. The goal of this control methodology is to bound the worst-case closed-loop performance of the process under study as measured by the induced 2-norm. Components of Figure 4 contained within the dashed line form the interconnection matrix, P, with the following state-space representation specific to the diabetic patient case study

Figure 4. Diabetic patient under H_∞ feedback control.

$$\begin{bmatrix} \begin{bmatrix} r-y \\ u_w \\ v \end{bmatrix} \end{bmatrix} = \begin{bmatrix} \begin{bmatrix} e_1 \\ e_2 \\ v \end{bmatrix} \end{bmatrix} = \begin{bmatrix} P_{11}(s) & P_{12}(s) \\ P_{21}(s) & P_{22}(s) \end{bmatrix} \begin{bmatrix} \begin{bmatrix} d_1 \\ d_2 \end{bmatrix} \\ u \end{bmatrix}$$

$$= \begin{bmatrix} A_p & B_d & B_u \\ \hline C_e & D_{ed} & D_{eu} \\ C_v & D_{vd} & D_{vu} \end{bmatrix} \begin{bmatrix} \begin{bmatrix} m_d \\ n \end{bmatrix} \\ u \end{bmatrix}. \quad (6)$$

The inputs were the meal disturbance, m_d, measurement noise, n, and the manipulated variable insulin infusion, u. System outputs were $r - y$, the error signal, u_w, the weighted input signal, and the plant measurement, v. The operator $P_{11}(s)$ captured the response of the output e signals in response to changes in the inputs d. This construction yielded the generalized block diagram system shown in Figure 5. An H_∞ controller, if one exists, minimizes $\| N \|_\infty$, defined as

$$\| N \|_\infty = \max_\omega \sigma \left[\mathcal{F}_l(P, K) \right] \quad (7)$$

$$\mathcal{F}_l(P, K) = P_{11} + P_{12} K (I - P_{22} K)^{-1} P_{21} \quad (8)$$

Figure 5. H_∞ synthesis problem.

Utilizing the theory of Doyle et al. (1989), several conditions must be satisfied to guarantee the existence of an H_∞ controller (Balas et al., 1995):

(1) (A_p, B_u) controllable and (A_p, C_v) detectable
(2) rank $(D_{eu}) = \dim(u)$ and rank $(D_{vd}) = \dim(v)$
(3) the following matrices must have full rank $\forall \omega$

$$\begin{bmatrix} A_p - j\omega I & B_u \\ C_e & D_{eu} \end{bmatrix} \text{ and } \begin{bmatrix} A_p - j\omega I & B_d \\ C_v & D_{vd} \end{bmatrix} \quad (9)$$

Assumption 1 simply states that the linearized reduced-order system must satisfy the controllability and observability criterion for linear systems based on the insulin delivery rate manipulated variable and arterial insulin concentration measurement. The second assumption guarantees a synthesized H_∞ controller is proper, and therefore realizable (Skogestad and Postlethwaite, 1996). Violation of this assumption leads to singular control problems (Balas et al., 1995). The final assumption is a mathematical technicality to ensure that the techniques in (Balas et al., 1995) are directly applicable. The conditions are relaxed forms of (C_d, A_p) detectable with $D_{eu}^T C_e = 0$ and (A_p, B_d) stabilizable with $B_d D_{vd} = 0$, respectively. For the system in the present study, these assumptions were satisfied. The system of two Riccati equations is solved through the γ-iteration technique utilizing the *hinfsyn* command in the μ-Tools toolbox (2000, MUSYN Inc. and The MathWorks, Inc.) of MATLAB (2000, The MathWorks, Inc.), which produces a nonunique suboptimal H_∞ controller.

Weighting function design

The controller design was completed by constructing the weighting functions in Figure 4: the input weight (W_u), meal disturbance weight (W_m), noise weight (W_n), and performance weight (W_p). The input weight was incorporated to provide column rank to the D_{12} matrix (D_{eu} in Eq. 6) when solving the nominal problem (plant = model = third order reduced linear model with no parameter variations). For systems which have been scaled such that their exogenous signals are less than unity magnitude, as the diabetic patient in this study has been, the weight $W_u = 1$ is reasonable (Skogestad and Postlethwaite, 1996). The choice of the scaling parameter, u_M, affects controller performance. A typical mechanical pump device for insulin delivery to a diabetic patient would be subject to the following magnitude constraint, which is conservative with respect to current pump literature (Minimed Corporation, 1999)

$$0 \, mU/\min \le \tilde{u}(k) \le 133 \, mU/\min \quad (10)$$

The maximum value, although not a mechanical constraint, was chosen to avoid severe over-delivery of insulin to diabetic patients. A controller design resulting from symmetric scaling about the nominal point (the typical method for H_∞ designs) with 0 mU/min and 44.6 mU/min bounds would prove highly conservative, as insulin delivery of $44.6 \le \tilde{u}(k) \le 133$ mU/min is within the constraints but would violate $|u| \le 1$. Note that this would be the easiest way to guarantee constraint satisfaction in H_∞ controller design for input constrained systems, however. At the other extreme, scaling u with $u_M = 133$ (the

typical disturbance scaling method) would allow utilization of the full manipulated variable range, but the calculation of negative insulin delivery rates, and the associated clipping at 0 mU/min, could lead to closed-loop instability. As an alternative to the above scaling methods, the input was scaled symmetrically using $u_M = 33.125$. This improves the disturbance rejection capability of the controller, while not radically altering the system stability properties.

Glucose meal disturbances were modeled as trapezoidal wave-forms (gastric emptying) followed by a first-order transfer function (absorption dynamics) (Lehmann and Deutsch, 1992). The transfer function was absorbed into G_m, along with the scaling value of 360 mg/min, which guaranteed that the input m_d would be bounded between $[0, 1]$. The deterministic disturbance signal affected the disturbance model with a time constant of approximately 6 minutes. A weighting function W_m was included to capture this dynamic behavior, with the following description:

$$W_m = \frac{1}{6s + 1} \quad (11)$$

This filter can be interpreted as an approximation of the trapezoidal rise, such that 5τ captured 99.3% of the response. The first-order roll-off was consistent with the disturbance signal effects, where higher frequency variations had a lesser effect on the disturbance model output.

The noise weight was included to account for any measurement noise effects in the glucose sensor. These effects were assumed white and Gaussian distributed. As the measurement noise did not have dynamics in this system, $W_n = constant$ was a convenient noise weight structure. This constant was 1/10000 for noise-free simulations, and was primarily included to impart full row rank in the D_{21} matrix (or D_{vd} in terms of Eq. 6) for the H_∞ controller calculation. For a study of measurement noise effects, noise weight adjustment was straightforward

$$W_n = \frac{\text{noise amplitude (mg/dL)}}{y \text{ scaling}}.$$

As described above, the system was subject to input constraints. Although there is no method to rigorously enforce constraints in the H_∞ design methodology, their effect on desired performance could be analyzed. Based on the input scaling, $|u| \le 1$, the available manipulated variable range was:

$$-10.8(\text{clipped to } 0) \le \tilde{u}(k) \le 66.25 \text{ mU/min}.$$

Acceptable control, as defined in (Skogestad and Postlethwaite, 1996), indicates whether sufficient manipulated variable action is present in the system to adequately reject disturbances. Mathematically, the criterion is

$$|G| > |G_m| - 1 \quad \forall \omega \text{ where } |G_m(\omega)| > 1, \quad (12)$$

where the transfer function G_m accounted for both the meal disturbance and measurement noise effects. The system satisfied the acceptable control criterion for the current variable

scaling. Therefore, a robust controller could be designed for this system based on the third order model, and input constraints should not saturate.

Performance weight selection is based on engineering judgment and the need to satisfy $(1/|W_p|) > |SG_mW_m| = |(1 + GK)^{-1}G_mW_m| \forall \omega$, where K is the H_∞ controller. The weighted sensitivity SG_mW_m was considered a good measure of the closed-loop performance in disturbance rejection scenarios. A straightforward choice for W_p is the first-order filter (Skogestad and Postlethwaite, 1996)

$$W_p(s) = \frac{\frac{s}{M} + \omega_b^*}{s + \omega_b^* A}. \qquad (13)$$

Disturbance rejection at steady state is governed by $A = 0.01$, and is chosen to make $|W_p|$ look like $|G_mW_m|$ at low frequency (Skogestad and Postlethwaite, 1996). Typically, M is taken as the least upper bound on the disturbance sensitivity, $\|SG_mW_m\|_\infty$. For the nominal problem, $M = 1.2$ was utilized. This was much larger than $\|SG_mW_m\|_\infty$, but allowed $(1/|W_p|) > |S|$, meaning that nominal performance in reference tracking was also guaranteed. The frequency, ω_b^*, was used as a tuning parameter to trade-off aggressiveness and robustness in the controller design. For the continuous-time nominal case, $\omega_b^* = 0.25$.

A similar procedure could be used in the case where uncertainty existed between the nominal model and the patient to be controlled. To represent the inter- and intra-patient variability, an input multiplicative uncertainty formulation was chosen. The modified block diagram representation is shown in Figure 6. The weights W_i and W_{im} were calculated as the least upper bound on the relative uncertainty of the perturbed plants, subject to the constraint that they were represented using low-order transfer functions. These weights were

$$W_i = \frac{s^2 + 0.47s + 0.015}{s^2 + 0.29s + 0.022} \qquad (14)$$

$$W_{im} = \frac{1.63s^2 + 0.21s + 0.007}{s^2 + 0.52s + 0.010}, \qquad (15)$$
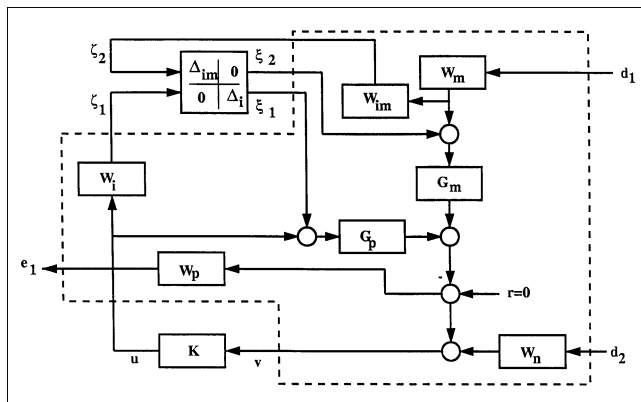
Figure 6. H_∞ problem, incorporating patient model uncertainty.
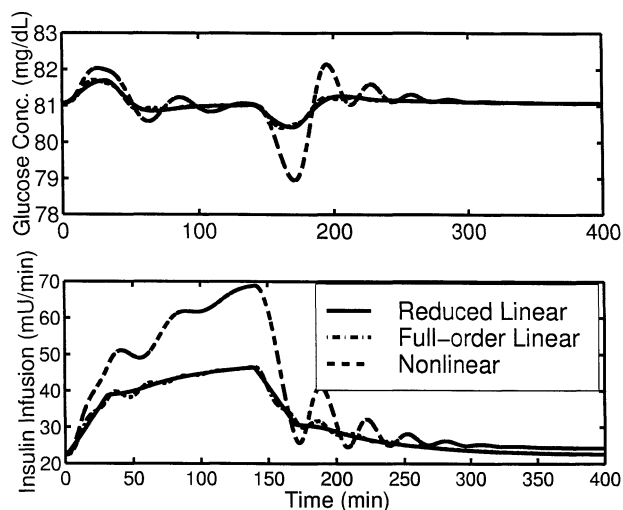
Figure 7. Nominal H_∞ controller applied to three patient models (no parametric uncertainty).

and the frequency domain plots are shown as the dashed lines in Figures 2 and 3, respectively. Also note that W_u was extraneous in the uncertainty formulation, and has been removed from the diagram.

Results

Continuous-time control

As a basis for further robust controller designs, a linear H_∞ controller was synthesized for the nominal problem using the weighting functions developed in the previous section and γ-iteration. The resulting controller had 5 states, and achieved a final γ value of $0.79 < 1$. This controller was applied to three patient models with no parametric uncertainty as an initial study in controller robustness. These models were: (i) the linear reduced-order model (three states); (ii) the linear full order model (19 states); and (iii) the nonlinear model. The diabetic patient models were subjected to a 50 g meal disturbance at time $t = 0$ min, and the resulting glucose concentration and insulin infusion profiles are shown in Figure 7. Similar to the work of Kienitz and Yoneyama (1993), this controller was tuned for performance in disturbance rejection. There was negligible performance degradation in the closed-loop response when model complexity was increased from third to nineteenth order (both linear), as the two curves nearly overlay. This was expected from the model reduction analysis, where the reduced model captured the full-order system behavior up to the bandwidth frequency of approximately 0.2 rad/min. Unless the linear full-order model under closed-loop control demonstrated significant time-domain differences from the reduced model, its profiles have been omitted from figures for the balance of this work. The over- and undershoot observed in controlling the nonlinear patient model were almost double that of the reduced model implementation, but the controller performance was quite reasonable, given that the deviations from the nominal case were located within the noise level of current glucose sensors (< 5 mg/dL). Based on the superior disturbance rejection and decreased insulin requirement for rejecting the meal dis-
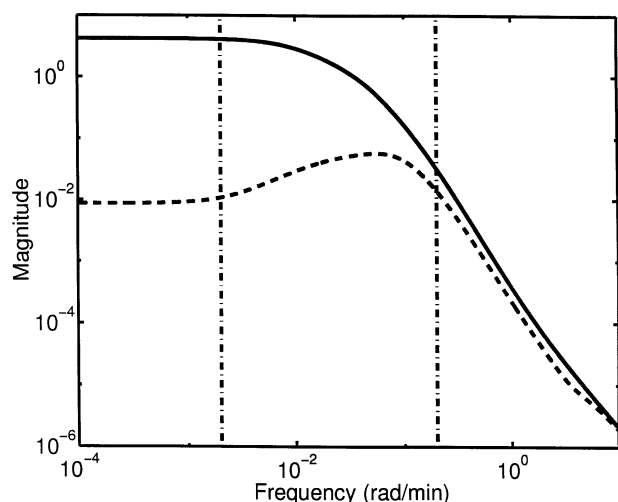
Figure 8. Frequency response: open-loop vs. closed-loop dynamics between *d* and *e*.

Solid: $|G_mW_m|$ (open-loop); dashed: $|SG_mW_m|$ (closed-loop). The bandwidth region is bounded by the dash-dot lines.

turbance, the two linear models predicted a patient with a greater sensitivity to insulin and a faster dynamic response to insulin delivery, as compared to the nonlinear patient model. This observation becomes important when analyzing robustness with respect to parametric variation.

As the disturbance signal has a non-unity gain on the controlled output, some additional interpretation for the γ parameter is necessary. The H_∞ design procedure constructs controllers with attenuation in the bandwidth region. This is illustrated in Figure 8 which displays the open- and closed-loop dynamics between d and e. The controller is synthesized from $|SG_mW_m|$, the weighted disturbance sensitivity, such that a value of $\gamma < 1$ implies $|e| < 1$, and hence satisfaction of the performance criteria.

As described in the section on Patient and Uncertainty Modeling, uncertainty was examined with respect to parameter values at three model locations. Incorporating the uncertainty weights W_i and W_{im} into the interconnection structure of Figure 6, a robust H_∞ controller was synthesized. The resulting controller had 13 states, performance weight parameters $A = 0.15$. $M = 2.5$, and $\omega_b^* = 0.002$, and satisfied $\gamma = 0.99 < 1$. As above, this controller was incorporated into three closed-loop systems, and these systems were subjected to the same 50 g meal disturbance. The resulting controller performance was quantified along with other controllers developed in the current work in Table 1. Clearly, there was a significant loss in performance when compared to the nominal case. This was a result of the controller detuning necessary to account for the potential uncertainty in the model. The performance was still reasonable, as the physiologically dangerous hypoglycemic condition, typically characterized as blood glucose values below 60 mg/dL (corresponding to undershoot in excess of 21.1 in Table 1), was avoided. The more important issue for this controller is the performance in the presence of parametric model uncertainty.

To analyze this parametric variation, a Monte Carlo technique was utilized. The effect of insulin on peripheral glucose uptake (EIPGU-D_Γ) and effect of glucose on hepatic

Table 1. Controller Performance Summary*

Controller Design	Overshoot (mg/dL)	Undershoot (mg/dL)	90% Settling Time (min)
	0.6	0.7	—
N	0.6	0.7	—
	1.1	2.1	—
	8.1	4.3	—
N-U	8.0	4.2	—
	11.7	7.9	163
	13.3	7.4	160
P-U	13.2	7.4	161
	24.6	16.9	339

*Controller designs are classified according to the letters in the first column. First letter describes the patient: (N)ominal model (no parameter variations) or uncertain (P)arameter model. Second letter describes the controller (if applicable): (U)ncertainty tuned controller. Rows within each section represent (1) the low-order patient model, (2) the full-order patient model, and (3) the nonlinear patient model.

glucose uptake (EGHGU-D_Γ) parameters were varied by $\pm 40\%$ in 20% increments from their nominal values of -5.82 and -1.48, respectively. The fractional hepatic insulin clearance (FHIC) was varied by $\pm 20\%$ in 10% increments from its nominal value of 0.4. This resulted in 125 possible perturbed patient models. The worst case performance (in terms of maximum deviation from the 81.1 mg/dL reference) is shown for the reduced-order linear and full-order nonlinear models in Figure 9. In the case of the reduced model, this corresponds to parameter values of EIPGU-$D_\Gamma = -8.15$, EGHGU-$D_\Gamma = 2.072$, and FHIC $= 0.48$. For the nonlinear patient models, the maximum glucose excursion was observed in the patient with FHIC $= 0.44$, and the minimum glucose value occurred for the patient with FHIC $= 0.36$ (EIPGU-$D_\Gamma = -8.15$, EGHGU-$D_\Gamma = -2.072$). Further performance degradation is observed, as detailed in Table 1. In all cases, this deviation from set point does not violate the hypoglycemic lower bound of 60 mg/dL.
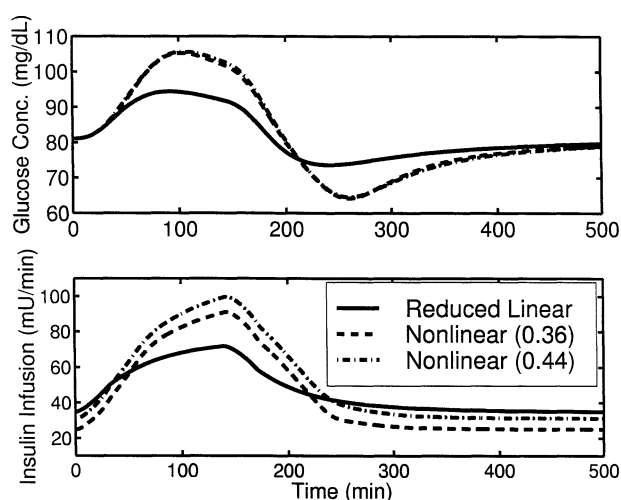

Figure 9. Worst case performance of the continuous-time H_∞ controller, including uncertainty weighting and parametric uncertainty.

Table 2. Performance Results for Meal Disturbance Simulations with Measurement Noise Applied to the Nonlinear Patient Model*

Controller Design	Overshoot (mg/dL)	Undershoot (mg/dL)	90% Settling Time (min)
N	11.9	8.0	356
	11.4	10.3	387
	12.3	13.1	393
N-U	9.3	2.7	151
	9.1	2.8	152
	13.5	5.0	174
P-U	16.4	4.6	177
	16.3	4.7	177
	30.5	12.7	336

*Controller abbreviations are identical to those in Table 1. Rows are (1) the low-order linear patient model, (2) the full-order linear patient model, and (3) the nonlinear patient model.

Measurement noise effects

Measurement noise will exist in any device, and in the H_∞ framework it is possible to account for a given level of noise explicitly in the controller synthesis. Noise of variance 2.0 [mg^2/dL^2] was included in the noise weight (W_n) for controller design and also on the measurement signal for the two controller formulations. The disturbance rejection results from the patient simulations are tabulated in Table 2. Each controller was detuned to accommodate noise, depending on the controller and patient model. The following adjustments were made to two performance parameters in the uncertain case: $\omega_b^* = 0.00075$; $A = 0.3$. Based on the relative performance of the nominal versus uncertain case, the uncertain controller was detuned to a much greater extent. The result is a greater tolerance to hyperglycemic excursion in the uncertain case, while the aggressive nominal case controller demonstrated similar excursions in the hyper- and hypoglycemic directions, respectively. As expected, performance degraded with respect to the noise-free simulations. Undershoot was acceptable for all controllers, as the hypoglycemic bound is not violated in any case. Note that although an overshoot value of greater than 20 is reported, this is for the nonlinear patient model, and is in the less dangerous hyperglycemic region. When using the linear reduced model, the error signal was less than unity for all t.

Unmodeled uncertainty

As the 3-parameter set which demonstrated the maximum average relative uncertainty (EIPGU-D_Γ, EGHGU-D_Γ, and FHIC) does not capture all parametric variations, a Monte Carlo technique was used to examine the effect of unmodeled parametric variation on controller performance. The 56 3-parameter sets were simulated in closed-loop, and 27 parametric variations were tested for each set: $+$max, no change, and $-$max for each parameter in the set in all combinations. This results in 577 unique patients. These patients were subjected to 50 g meal disturbances at time $t = 0$ under closed-loop control by the uncertainty-tuned controller. A typical result is shown in Figure 10. This patient had the following parameter variations from a nominal of 1.0: EIPGU-$E_\Gamma = 0.6$, EGHGU-$E_\Gamma = 0.6$, EGHGP-$E_\Gamma = 1.4$. This represents a pa-
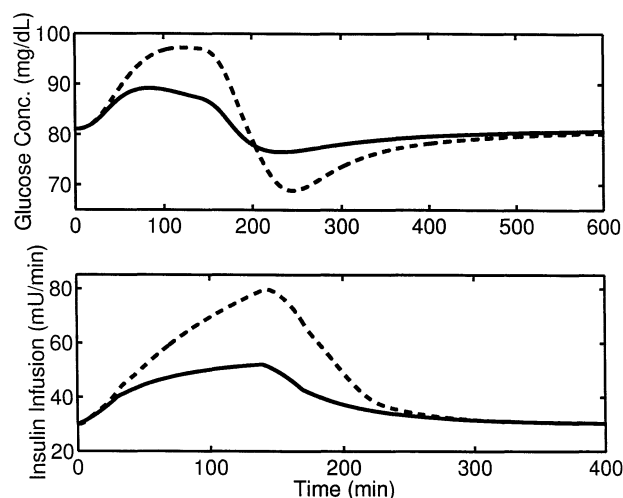

Figure 10. Closed-loop H_∞ control of an uncertain patient with mismatched dynamics.

Solid: reduced-order model; dashed: nonlinear model. A 50 g meal disturbance is introduced at time $t = 0$. Patient parameters are: EIPGU-$E_\Gamma = 0.6$, EGHGU-$E_\Gamma = 0.6$, EGHGP-$E_\Gamma = 1.4$ (all have nominal value 1.0).

tient who has insulin resistant peripheral tissue and a glucose resistant liver. As would be expected from a robust controller, the 50 g meal disturbance was successfully rejected while keeping the arterial glucose concentration within the expected range (-12.2 mg/dL to $+16.2$ mg/dL for the *nonlinear* patient). The settling time for this patient is reasonable as well (294 min), when compared to the controller performance in Table 1. All reduced-order and full-order linear patient models satisfied the performance bounds. It should be noted, however, that of the 577 nonlinear patients tested, there were 72 who violated the performance results (12%) and entered the dangerous hypoglycemic region. Of these patients, one had a parameter combination yielding disturbance relative uncertainty > 1 at steady-state, and the balance had FPIC = 0.225. Clearly, the nonlinear effects of this parameter are significant, and its value must be estimated prior to controller implementation. Otherwise, the closed-loop performance on uncertain nonlinear patients was within the prespecified performance region.

Discussion
Existing literature results

The present results are compared to the results of Kienitz and Yoneyama (1993), who developed an H_∞ controller based on a third order linear diabetic patient model. Performance of their controller in response to a meal disturbance (albeit of different shape) was quantitatively similar to the nominal controller shown in Figure 7. The uncertainty-derived controller from the present work demonstrated greater over- and undershoot, but it was tuned to handle significantly more uncertainty than the literature controller. To characterize uncertainty, (Kienitz and Yoneyama, 1993) varied the parameters to the model by $\pm 50\%$ of their nominal value (the A_{21} parameter varied over $[0, 0.025]$). An analysis of relative uncertainty, similar to that of Figure 2 and omitted in their de-

sign, resulted in certain parameter combinations having magnitude greater than unity at low frequency (steady-state). This indicates that some members of the perturbed model set may have a different steady-state gain than the actual process, and one could not construct an H_∞ controller for this process. They circumvented the large uncertainties by adding additional tuning blocks to their controller design, such that the uncertainty block (represented by Δ_i and Δ_{im} in the current work) was weighted by 0.01 over all frequencies. This analysis effectively neglected uncertainty (maximum relative uncertainty over all frequencies was less than 8%) and instead concentrated on performance in disturbance rejection scenarios. The present study instead examined closed-loop behavior in the presence of significant model uncertainty and structural mismatch, while satisfying the performance bounds of the H_∞ problem.

Model predictive control

Another approach to controlling glucose in diabetic patients is model predictive control (MPC) (Parker et al., 1999a; Trajanoski et al., 1997, 1998). To evaluate the performance of an MPC controller versus the robust control approaches detailed here, two cases are examined. The nominal controller is compared to an MPC controller for 50 g meal disturbance rejection in the nominal *nonlinear* patient. The glucose and insulin profiles can be found in Figure 11. Small over- and undershoot is observed, as well as rapid settling times. The H_∞ algorithm is superior in terms of reference tracking, with approximately a 91% reduction in sum-squared error. However, this is expected as the H_∞ algorithm operates in continuous time, while MPC algorithms are inherently discrete. Overall, the performance of both control algorithms is excellent.

Controller performance degrades when uncertainty is present, as observed for the H_∞ controllers in Figure 9. To
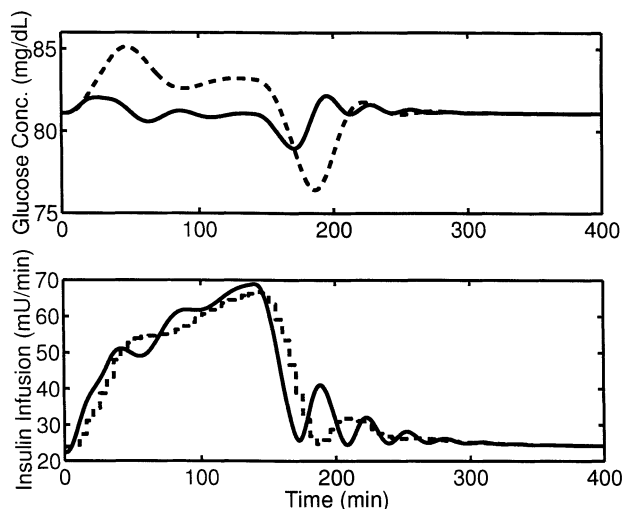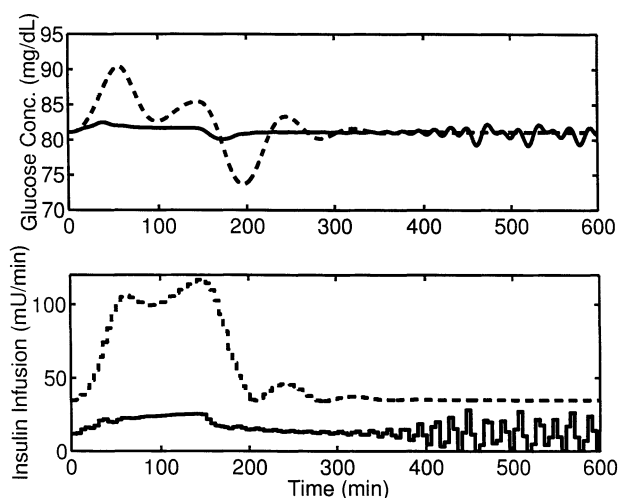
Figure 12. Performance of the state-estimating MPC controller [tuning parameters same as above] rejecting a 50 g meal disturbance in uncertain nonlinear patients.

Patient parameters are: EIPGU-D_Γ = −3.493678, EGHGU-D_Γ = −0.888, FHIC = 0.32 (solid); EIPGU-D_Γ = −8.149582, EGHGU-D_Γ = −2.072, FHIC = 0.48 (dashed).

further analyze the differences in performance between H_∞ control and MPC for the diabetes problem, the 27 combinations of the EIPGU-D_Γ/EGHGU-D_Γ/FHIC parameter set were simulated. Two results are shown in Figure 12. These patients have parameter values EIPGU-D_Γ = −3.493678, EGHGU-D_Γ = −0.888, FHIC = 0.32 (solid) and EIPGU-D_Γ = −8.149582, EGHGU-D_Γ = −2.072, FHIC = 0.48 (dashed). These patients are highly insulin sensitive (solid) or resistant (dashed). The MPC controller performance in terms of glucose tracking is superior to the H_∞ algorithms, although some oscillation is evident. Insulin resistant patients are handled by delivering more insulin, but the MPC controller has difficulty stabilizing for insulin sensitive patients because it is too aggressive. The addition of parameter estimation to the control algorithm may alleviate some of the performance problems, but at the same time other issues such as mismatched dynamics and the aggressiveness of the update mechanism arise.

Conclusions

H_∞ optimal design of an insulin infusion pump controller requires an accurate yet low order process description, as well as a characterization of the potential uncertainties which may exist in the system. Uncertainty within the reduced model, derived from physiological conditions within the nonlinear representation, was characterized in a control-relevant manner using relative uncertainty. Nominal controller performance is shown to be similar to those published in earlier literature, and a more thorough analysis of robustness to model uncertainty is presented. Continuous-time H_∞ controllers perform well for modeled uncertainty, and the closed-loop relevance of the uncertainty characterization is validated by the adequate performance of almost 90% of unmodeled

Figure 11. Performance: nominal H_∞ controller (solid) vs. MPC (dashed).

[MPC tuning parameters: sample time = 5 min, move horizon = 2, prediction horizon = 8, reference filter = 0.65] in rejecting a 50 g meal disturbance to the nominal nonlinear patient.

parametric variations. For those cases where performance was not acceptable, a single parameter is responsible. The H_∞ controller was shown to have comparable performance to the more complex MPC algorithm (in terms of on-line computation). Robustness to parameter variations is evident, while the MPC algorithm had some stabilization problems. For tracking performance, however, the MPC algorithm significantly reduced over- and undershoot, such that a parameter estimating linear MPC algorithm may overcome the stabilization problems. The selection of a control algorithm is clearly a multi-objective problem where H_∞ and MPC approaches have their individual advantages and shortcomings.

Acknowledgments

Literature Cited

Ackerman, E., L. C. Gatewood, J. W. Rosevear, and G. D. Molnar, "Model Studies of Blood-Glucose Regulation," *Bull. Mathem. Biophys.*, **27**(Suppl.), 21 (1965).

Ashcroft, F. M., and S. J. H. Ashcroft, *Insulin: Molecular Biology to Pathology*, Oxford University Press, New York (1992).

Balas, G. J., J. Doyle, K. Glover, A Packard, and R. Smith, *μ-Analysis and Synthesis Toolbox User's Guide*, The Mathworks, Natick, MA (1995).

Bergman, R. N., L. S. Phillips, and C. Cobelli, "Physiologic Evaluation of Factors Controlling Glucose Tolerance in Man," *J. Clin. Invest.*, **68**, 1456 (1981).

Bolie, V. W., "Coefficients of Normal Blood Glucose Regulation," *J. Appl. Physiol.*, **16**, 783 (1961).

Bremer, T., and D. A. Gough, "Is Blood Glucose Predictable From Previous Values? A Solicitation for Data," *Diabetes*, **48**, 445 (1999).

Chiang, R. Y., and M. G. Safonov, *Robust Control Toolbox*, The Mathworks, Inc., Natick, MA (1992).

Cobelli, C., and A. Mari, "Validation of Mathematical Models of Complex Endocrine-Metabolic Systems. A Case Study on a Model of Glucose Regulation," *Med. Biol. Eng. Comput.*, **21**, 390 (1983).

Cohen, A., "New Disposable Electronic Micropump for Parenteral Drug Delivery," R. Gurny, H. E. Junginger, and N. A. Peppas, eds., *Pulsatile Drug Delivery: Current Applications and Future Trends*, Wissenschaftliche, Stuttgart, Germany, p. 151 (1993).

Doyle, J. C., K. Glover, P. P. Khargonekar, and B. A. Francis, "State-Space Solutions to Standard H_2 and H_∞ Control Problems," *IEEE Trans. Aut. Control*, **34**, 831 (1989).

Fisher, M. E., "A Semiclosed-Loop Algorithm for the Control of Blood Glucose Levels in Diabetics," *IEEE Trans. Biomed. Eng.*, **38**, 57 (1991).

Glover, K., "All Optimal Hankel Norm Approximations of Linear Multivariable Systems, and Their L_∞-Error Bounds," *Int. J. Control*, **39**, 1145 (1984).

Guyton, J. R., R. O. Foster, J. S. Soeldner, M. H. Tan, C. B. Kahn, L. Koncz, and R. E. Gleason, "A Model of Glucose-Insulin Homeostasis in Man that Incorporates the Heterogeneous Fast Pool Theory of Pancreatic Insulin Release," *Diabetes*, **27**, 1027 (1978).

Kienitz, K. H., and T. Yoneyama, "A Robust Controller for Insulin Pumps Based on H-Infinity Theory," *IEEE Trans. Biomed. Eng.*, **40**, 1133 (1993).

Lehmann, E. D., and T. Deutsch, "A Physiological Model of Glucose-Insulin Interaction in Type 1 Diabetes Mellitus," *J. Biomed. Eng.*, **14**, 235 (1992).

Meyerhoff, C., F. Bischof, F. Sternberg, H. Zier, and E. F. Pfeiffer, "On Line Continuous Monitoring of Subcutaneous Tissue Glucose

in Men by Combining Portable Glucosensor with Microdialysis," *Diabetologia*, **35**, 1087 (1992).

Minimed Corp, *The Minimed 507C, Products and Specifications*, http://www. minimed.com/files/mm_098.htm (1999).

Moore, B. C., "Principal Component Analysis in Linear Systems: Controllability, Observability, and Model Reduction," *IEEE Trans. Aut. Control*, **AC-26**, 17 (1981).

Morari, M., "Robust Stability of Systems with Integral Control," Proc. of IEEE Conf. on Decision and Control, San Antonio, TX, IEEE Press, Piscataway, NJ, p. 865 (1983).

Nishida, K., M. Sakakida, K. Ichinose, T. Uemura, M. Uehara, K. Kajiwara, T. Miyata, M. Shichiri, K. Ishihara, and N. Nakabayashi, "Development of a Ferrocene-Mediated Needle-Type Glucose Sensor Covered with Newly Designed Biocompatible Membrane, 2-Methacryloyloxyethylphosphorylcholine-co-n-Butyl Methacrylate," *Med. Prog. Technol.*, **21**, 91 (1995).

Ollerton, R. L., "Application of Optimal Control Theory to Diabetes Mellitus," *Int. J. Control*, **50**, 2503 (1989).

Parker, R. S., *Model-Based Analysis and Control for Biosystems*, PhD thesis, Dept. of Chemical Engineering, University of Delaware (1999).

Parker, R. S., F. J. Doyle III, and N. A. Peppas, "Uncertainty and Robustness in Diabetic Patient Blood Glucose Control," *AIChE Meeting*, Miami (1998).

Parker, R. S., F. J. Doyle III, and N. A. Peppas, "A Model-Based Algorithm for Blood Glucose Control in Type I Diabetic Patients," *IEEE Trans. Biomed. Eng.*, **46**, 148 (1999a).

Parker, R. S., A. T. Stamps, N. A. Peppas, and F. J. Doyle III, "Robust H_∞ Control of Type I Diabetic Patient Blood Glucose," paper No. 266b, *AIChE Meeting*, Dallas (1999b).

Preidel, W., S. Saeger, I. Von Lucadou, and W. Lager, "An Electrocatalytic Glucose Sensor for In-Vivo Application," *Biomed. Instrum. Technol.*, **25**, 215 (1991).

Puckett, W. R., and E. N. Lightfoot, "A Model for Multiple Subcutaneous Insulin Injections Developed from Individual Diabetic Patient Data," *Am. J. Physiol.*, **269** (**Endocrinol. Metab. 32**), E1115 (1995).

Simon, G., G. Brandenberger, and M. Follenius, "Ultradian Oscillations of Plasma Glucose, Insulin, and C-Peptide in Man During Continuous Enteral Nutrition," *J. Clin. Endocrinol. Metab.*, **64**, 669 (1987).

Skogestad, S., and I. Postlethwaite, *Multivariable Feedback Control*, Wiley, New York (1996).

Sorensen, J. T., "A Physiologic Model of Glucose Metabolism in Man and its Use to Design and Assess Improved Insulin Therapies for Diabetes," PhD Thesis, Dept. of Chemical Engineering, MIT (1985).

Steil, G. M., J. Murray, R. N. Bergman, and T. A. Buchanan, "Repeatability of Insulin Sensitivity and Glucose Effectiveness from the Minimal Model—Implications for Study Design," *Diabetes*, **43**, 1365 (1994).

Trajanoski, Z., W. Regittnig, and P. Wach, "Neural Predictive Controller for Closed-Loop Control of Glucose using the Subcutaneous Route: A Simulation Study," *Chem. Eng. Prog.*, **5**, 1727 (1997).

Trajanoski, Z., W. Regittnig, and P. Wach, "Simulation Studies on Neural Predictive Control of Glucose using the Subcutaneous Route," *Comp. Method. Program. Biomed.*, **56**, 133 (1998).

Appendix: Diabetic Patient Model

The following notation is used throughout the model description:

Model variables:

A = auxiliary equation state (dimensionless)
B = fractional clearance (I, dimensionless; N, L/min)
G = glucose concentration (mg/dL)
I = insulin concentration (mU/L)
N = glucagon concentration (normalized, dimensionless)
Q = vascular plasma flow rate (L/min)
q = vascular blood flow rate (dL/min)
T = transcapillary diffusion time constant (min)
V = volume (L)

v = volume (dL)
Γ = metabolic source or sink rate (mg/min or mU/min)

Glucose Model Sub- and Superscripts

A = hepatic artery
B = brain
BU = brain uptake
C = capillary space
G = glucose
H = heart and lungs
HGP = hepatic glucose production
HGU = hepatic glucose uptake
I = insulin
$IHGP$ = insulin effect on HGP
$IHGU$ = insulin effect on HGU
IVI = intravenous insulin infusion
K = kidney
KC = kidney clearance
KE = kidney excretion
L = liver
LC = liver clearance
N = glucagon
$NHGP$ = glucagon effect on HGP
P = periphery (muscle/adipose tissue)
PC = peripheral clearance
PGU = peripheral glucose uptake
PIR = pancreatic insulin release
PNC = pancreatic glucagon clearance
PNR = pancreatic glucagon release (normalized)
$RBCU$ = red blood cell uptake
S = gut (stomach/intestine)
SIA = insulin absorption into blood stream from subcutaneous depot
SU = gut uptake
T = tissue space

The human glucose-insulin system model used in this study was based on initial work by Guyton et al. (1978) which was updated by Sorensen (1985). The current work modified the Sorensen model to include generalized meal disturbances as well as parameters for uncertainty analysis. Utilizing compartmental modeling techniques, the diabetic patient model is represented schematically in Figure A1. Individual com-
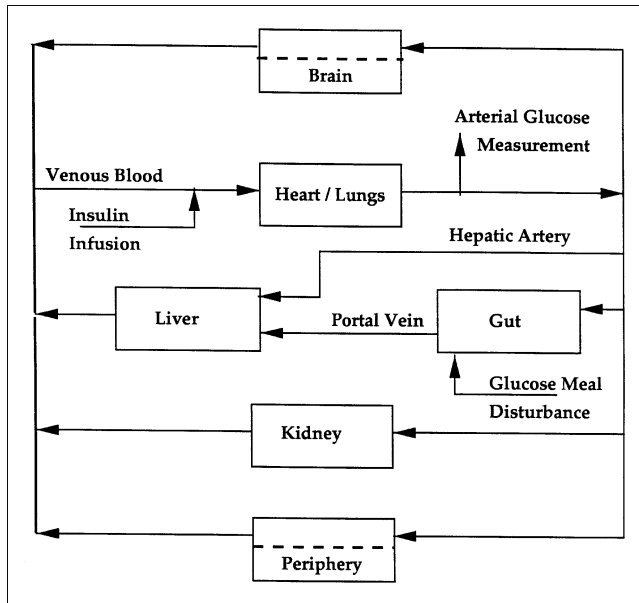
Figure A1. Compartmental diagram of the glucose and insulin systems in a diabetic patient.

partment models were obtained by performing mass balances around tissues important to glucose or insulin dynamics. This resulted in a six-compartment representation, where the compartmentalized organs were the brain, heart/lungs, gut, liver, kidney, and periphery. In the context of this model, the periphery represents the combined effects of muscle and adipose tissue while the stomach and intestine effects are lumped into the gut compartment. Blood transported glucose or insulin to the various compartments via convection. It was assumed that the glucose or insulin concentration in a compartment was in equilibrium with the blood leaving the given compartment. Once in a particular compartment, glucose and insulin were either metabolized or transported via diffusion to a tissue subcompartment. Subcompartments, such as those in the brain and periphery, were only included where significant resistance to diffusion (such as time delay or equilibration time) existed. Subcompartments were not necessary if the tissue group did not absorb the material of interest or the tissue concentration equilibrated rapidly with the blood. For tissues with subcompartments, glucose and insulin metabolism were assumed to take place within the tissue (as opposed to the capillary) subcompartment.

The glucose submodel differential mass balance equations are given by:

$$\dot{G}_B^C = \left(G_H^C - G_B^C \right) \frac{q_B}{v_B^C} - \left(G_B^C - G_B^T \right) \frac{v_B^T}{T_B v_B^C} \tag{A1}$$

$$\dot{G}_B^T = \left(G_B^C - G_B^T \right) \frac{1}{T_B} - \frac{\Gamma_{BU}}{v_B^T} \tag{A2}$$

$$\dot{G}_H^C = \left(G_B^C q_B + G_L^C q_L + G_K^C q_K + G_P^C q_P - G_H^C q_H - \Gamma_{RBCU} \right) \frac{1}{v_H^C} \tag{A3}$$

$$\dot{G}_S^C = \left(G_H^C - G_S^C \right) \frac{q_S}{v_S^C} + \frac{\Gamma_{\text{meal}}}{v_S^C} - \frac{\Gamma_{SU}}{v_S^C} \tag{A4}$$

$$\dot{G}_L^C = \left(G_H^C q_A + G_S^C q_S - G_L^C q_L \right) \frac{1}{v_L^C} + \frac{\Gamma_{HGP}}{v_L^C} - \frac{\Gamma_{HGU}}{v_L^C} \tag{A5}$$

$$\dot{G}_K^C = \left(G_H^C - G_K^C \right) \frac{q_K}{v_K^C} - \frac{\Gamma_{KE}}{v_K^C} \tag{A6}$$

$$\dot{G}_P^C = \left(G_H^C - G_P^C \right) \frac{q_P}{v_P^C} + \left(G_P^T - G_P^C \right) \frac{v_P^T}{T_P^G v_P^C} \tag{A7}$$

$$\dot{G}_P^T = \left(G_P^C - G_P^T \right) \frac{1}{T_P^G} - \frac{\Gamma_{PGU}}{v_P^T} \tag{A8}$$

where

$$k_B^C = G_B^C \frac{v_B^T}{T_B}$$

$$k_B^T = G_B^T \frac{v_B^T}{T_B}$$

The metabolic source and sink terms ($\Gamma_i \, [=] \,$ mg/min) in the

above equations were defined by

$$\Gamma_{BU} = 70 \tag{A9}$$

$$\Gamma_{RBCU} = 10 \tag{A10}$$

$$\Gamma_{SU} = 20 \tag{A11}$$

$$\Gamma_{HGP} = 155 A_{IHGP}\left[2.7\tanh\left(0.388N\right) - A_{NHGP}\right]$$
$$\times \left[1.425 - 1.406\tanh\left\{0.6199\left(\frac{G_L^C}{101} - 0.4969\right)\right\}\right] \tag{A12}$$

$$\dot{A}_{IHGP} = \frac{1}{25}\left[1.2088 - 1.138\tanh\left(1.669\frac{I_L^C}{21.43} - 0.8885\right)\right.$$
$$\left. - A_{IHGP}\right] \tag{A13}$$

$$\dot{A}_{NHGP} = \frac{1}{65}\left[\frac{2.7\tanh\left(0.388N\right) - 1}{2} - A_{NHGP}\right] \tag{A14}$$

$$\Gamma_{HGU} = 20 A_{IHGU}\left[5.6648 + 5.6589\tanh\left\{2.4375\left(\frac{G_L^C}{101}\right.\right.\right.$$
$$\left.\left.\left. - 1.48\right)\right\}\right] \tag{A15}$$

$$\dot{A}_{IHGU} = \frac{1}{25\,\text{min}}\left[2\tanh\left(0.549\frac{I_L^C}{21.43}\right) - A_{IHGU}\right] \tag{A16}$$

$$\Gamma_{KE}$$
$$= \begin{cases} 71 + 71\tanh\left[0.011\left(G_K^C - 460\right)\right] & \text{for } G_K^C < 460\ \text{mg/dL} \\ 0.872 G_K^C - 300 & \text{for } G_K^C \geq 460\ \text{mg/dL} \end{cases} \tag{A17}$$

$$\Gamma_{PGU}$$
$$= \frac{35 G_P^T}{86.81}\left[7.035 + 6.51623\tanh\left\{0.33827\left(\frac{I_P^T}{5.304} - 5.82113\right)\right\}\right]. \tag{A18}$$

The insulin submodel mass balances were given by

$$\dot{I}_B^C = \left(I_H^C - I_B^C\right)\frac{Q_B}{V_B^C} \tag{A19}$$

$$\dot{I}_H^C = \left(I_B^C Q_B + I_L^C Q_L + I_K^C Q_K + I_P^C Q_P - I_H^C Q_H - \Gamma_{IVI}\right)\frac{1}{V_H^C} \tag{A20}$$

$$\dot{I}_S^C = \left(I_H^C - I_S^C\right)\frac{Q_S}{V_S^C} \tag{A21}$$

$$\dot{I}_L^C = \left(I_H^C Q_A + I_S^C Q_S - I_L^C Q_L\right)\frac{1}{V_L^C} + \frac{\Gamma_{PIR} - \Gamma_{LC}}{V_L^C} \tag{A22}$$

$$\dot{I}_K^C = \left(I_H^C - I_K^C\right)\frac{Q_K}{V_K^C} - \frac{\Gamma_{KC}}{V_K^C} \tag{A23}$$

$$\dot{I}_P^C = \left(I_H^C - I_P^C\right)\frac{Q_P}{V_P^C} - \left(I_P^C - I_P^T\right)\frac{V_P^T}{T_P^I V_P^C} \tag{A24}$$

$$\dot{I}_R^T = \left(I_P^C - I_P^T\right)\frac{1}{T_P^I} + \frac{\Gamma_{SIA} - \Gamma_{PC}}{V_P^T}. \tag{A25}$$

The related metabolic sinks ($\Gamma_i\ [=]\ \text{mU/min}$) were

$$\Gamma_{LC} = F_{LC}\left(I_H^C Q_A + I_S^C Q_S + \Gamma_{PIR}\right) \tag{A26}$$

$$\Gamma_{PIR} = 0, \text{ no pancreatic insulin release} \tag{A27}$$

$$\Gamma_{KC} = F_{KC} I_K^C Q_K \tag{A28}$$

$$\Gamma_{PC} = \frac{I_P^T}{\dfrac{1 - F_{PC}}{F_{PC}}\dfrac{1}{Q_P} - \dfrac{1}{T_P^I V_P^T}}. \tag{A29}$$

Glucagon, the potentiator responsible for stimulating glucose release into the bloodstream, was modeled as a single blood pool compartment governed by the mass balance

$$\dot{N} = \left(\Gamma_{PNR} - N\right)\frac{F_{PNC}}{V_N}. \tag{A30}$$

Glucagon release from the α-cells of the pancreas ($\Gamma_i\ [=]\ \mu\text{g/min}$) was

$$\Gamma_{PNR} = \left[1.3102 - 0.61016\tanh\left\{1.0571\left(\frac{I_H^C}{15.15} - 0.46981\right)\right\}\right]$$
$$\times \left[2.9285 - 2.095\tanh\left\{4.18\left(\frac{G_H^C}{91.89} - 0.6191\right)\right\}\right]. \tag{A31}$$

Overall, the diabetic patient was characterized by nineteen differential equations, with eleven describing glucose dynamics, seven for insulin dynamics, and a single compartment for glucagon. Model parameters are as shown in Table A1.

Appended to the diabetic patient model was a generalized meal model, as presented by Lehmann and Deutsch (1992).

Table A1. Parameter Values for the Diabetic Patient

$v_B^C = 3.5$ dL	$q_B = 5.9$ dL/min	$T_B = 2.1$ min
$v_B^T = 4.5$ dL		
$v_H^C = 13.8$ dL	$q_H = 43.7$ dL/min	
$v_S^C = 11.2$ dL	$q_S = 10.1$ dL/min	
$v_L^C = 25.1$ dL	$q_L = 12.6$ dL/min	
	$q_A = 2.5$ dL/min	
$v_K^C = 6.6$ dL	$q_K = 10.1$ dL/min	
$v_P^C = 10.4$ dL	$q_P = 15.1$ dL/min	$T_P^G = 5.0$ min
$v_P^T = 67.4$ dL		
$V_B^C = 0.265$ L	$Q_B = 0.45$ L/min	
$V_H^C = 0.985$ L	$Q_H = 3.12$ L/min	
$V_S^C = 0.945$ L	$Q_S = 0.72$ L/min	
$V_L^C = 1.14$ L	$Q_L = 0.9$ L/min	
	$Q_A = 0.18$ L/min	
$V_K^C = 0.505$ L	$Q_K = 0.72$ L/min	
$V_P^C = 0.735$ L	$Q_P = 1.05$ L/min	$T_P^I = 20$ min
$V_P^T = 6.3$ L		
$V_N = 9.93$ L	$F_{PNC} = 0.910$ L/min	

Table A2. Nominal Values for Uncertain Parameters in the Diabetic Patient Model

EIPGU-$E = 1.0$	EGHGU-$E = 1.0$	EGHGP-$E = 1.0$
EIPGU-$D = -5.82113$	EGHGU-$D = -1.48$	EGHGP-$D = -0.4969$
FHIC (F_{LC}) $= 0.4$	FPIC (F_{PC}) $= 0.15$	

This representation modeled gastric emptying of carbohydrate as a saturating function (with maximum rate of 360 mg/min carbohydrate) to maintain relatively constant carbohydrate release from the stomach during intestinal adsorption. The rise to and fall from this maximum rate was a linear function (ramp), taking place over a thirty minute span. Small meals (< 10.2 g carbohydrate) only contained the rise and fall phases (triangle shape), never reaching the plateau emptying rate. Larger meals were described by a trapezoidal wave. Either gastric emptying function was followed by the following first-order filter

$$\Gamma_{\text{meal}} = \frac{1/60}{s + 1/60} wf, \qquad (A32)$$

where Γ_{meal} represents the absorption rate of glucose into the diabetic patient model gut compartment and wf was the input waveform signal.

The uncertainty analysis utilizes 8 parameters from the above model. These are located in the following relations

$$\Gamma_{EIPGU} = 1.0 \left\{ 7.035 + 6.51623 \tanh \left[0.33827 \left(\frac{I_P^T}{5.304} - 5.82113 \right) \right] \right\} \qquad (A33)$$

$$\Gamma_{EGHGU} = 1.0 \left\{ 5.6648 + 5.6589 \tanh \left[2.4375 \left(\frac{G_L^C}{101} - 1.48 \right) \right] \right\} \qquad (A34)$$

$$\Gamma_{EGHGP} = 1.0 \left\{ 1.425 - 1.406 \tanh \left[0.6199 \left(\frac{G_L^C}{101} - 0.4969 \right) \right] \right\} \qquad (A35)$$

$$\Gamma_{LC} = F_{LC} \left(I_H^C Q_A + I_S^C Q_S + \Gamma_{PIR} \right) \qquad (A36)$$

$$\Gamma_{PC} = \frac{I_P^T}{\frac{1 - F_{PC}}{F_{PC}} \frac{1}{Q_P} - \frac{1}{T_P^I V_P^T}}. \qquad (A37)$$